Research in Astronomy and Astrophysics, 24:115011 (7pp), 2024 November https://doi.org/10.1088/1674-4527/ad8627

Jets, Accretion and Spin in Supermassive Black Holes

Yongyun Chen[1,2], Qiusheng Gu[2,3], Jianghe Yang[4], Junhui Fan[5], Xiaoling Yu[1], Dingrong Xiong[6], Nan Ding[7], and Xiaotong Guo[8]
[1] College of Physics and Electronic Engineering, Qujing Normal University, Qujing 655011, China; ynkmcyy@yeah,net
[2] School of Astronomy and Space Science, Nanjing University, Nanjing 210093, China; qsgu@nju.edu.cn
[3] Key Laboratory of Modern Astronomy and Astrophysics (Nanjing), Ministry of Education, Nanjing 210093, China
[4] College of Mathematics and Physics Science, Hunan University of Arts and Science, Changde 415000, China
[5] Center for Astrophysics, Guangzhou University, Guangzhou 510006, China
[6] Yunnan Observatories, Chinese Academy of Sciences, Kunming 650011, China
[7] School of Physical Science and Technology, Kunming University, Kunming 650214, China
[8] Institute of Astronomy and Astrophysics, Anqing Normal University, Anqing 246133, China
Received 2024 June 6; revised 2024 September 11; accepted 2024 October 8; published 2024 November 6

Abstract

The theoretical model suggests that relativistic jets of active galactic nuclei (AGNs) rely on the black hole spin and/or accretion. We study the relationship between jet, accretion, and spin using supermassive black hole samples with reliable spin of black holes. Our results are as follows: (1) There is a weak correlation between radio luminosity and the spin of the black hole for our sample, which may imply that the jet of the supermassive black hole in our sample depends on the other physical parameters besides black hole spins, such as accretion disk luminosity. (2) The jet power of a supermassive black hole can be explained by the hybrid model with magnetic field of corona. (3) There is a significant correlation between radio-loudness and black hole spin for our sample. These sources with high radio-loudness tend to have high black hole spins. These results provide observational evidence that the black hole spin may explain the bimodal phenomena of radio-loud and radio-quiet AGNs.

Key words: galaxies: active – galaxies: general – galaxies: jets

1. Introduction

The origin of jets from active galactic nuclei (AGNs) has always been unclear. It is generally believed that the origin of jets is mainly related to accretion and the spin of a supermassive black hole (e.g., Blandford & Znajek 1977; Ghisellini 2006; Zamaninasab et al. 2014). Some authors have suggested that the power of jets is closely linked to the accretion disk luminosity (e.g., Rawlings & Saunders 1991; Ghisellini et al. 2014; Sbarrato et al. 2014; Chen et al. 2015a, 2015b; Paliya et al. 2017; Chen et al. 2023a, 2023b, 2023c). Ghisellini et al. (2014) found that the power of jets is greater than the luminosity of the accretion disk, which implies that the spin of black holes may play an important role in the formation of jets besides accretion. Some authors have found that the jets of stellar mass black holes in X-ray binaries are related to the black hole spin (Narayan & McClintock 2012; Steiner et al. 2013). Recently, Cui et al. (2023) found a precessing jet nozzle connecting to a spinning black hole in M87. This result may suggest that the jet is closely related to the spin of the black hole. However, Fender et al. (2010) found that there was no correlation between the spin of black holes and jets in X-ray binaries. Although there are some studies on the relationship between black hole spin and jet. However, whether the black hole spin enhances the relativistic jets has not been studied by using large samples with reliable black hole spins.

The origin of the dichotomy of radio-quiet and radio-loud AGNs has been discussed in the literature. Some authors suggest that the accretion rate (Eddington ratios $\lambda = L_{\rm bol}/L_{\rm Edd}$, where $L_{\rm bol}$ is the bolometric luminosity and $L_{\rm Edd}$ is the Eddington luminosity) may explain this bimodal phenomenon (e.g., Ho et al. 2000; Sikora et al. 2007). Another possible explanation is that the black hole spin leads to the dichotomy phenomenon of radio-loud and radio-quiet AGNs. Recently, Sikora et al. (2007) discovered that radio-loud AGN is hosted in elliptical galaxies, while radio-quiet AGN is likely hosted in spiral galaxies. Volonteri et al. (2007) found that spiral galaxies have lower spin of black holes than elliptical galaxies. This result indicates that the dichotomy of radio-loud and radio-quiet AGNs can be explained by the supermassive black hole spin. However, there is currently a lack of observational evidence to support the correlation between black hole spin and radio-loudness.

In this paper, we mainly study the relationship between jet and black hole spin and accretion by using large samples. We also study the relationship between black hole spin and radio-loudness. The sample is presented in Section 2; the jet model is described in Section 3; Section 4 presents the results and discussion; Section 5 describes the conclusions. A ΛCDM cosmology with $H_0 = 70\,{\rm km\,s^{-1}\,Mpc^{-1}}$, $\Omega_m = 0.27$, $\Omega_\Lambda = 0.73$ is adopted.

2. The Sample

2.1. The Sample of Supermassive Black Holes

We select a large sample of supermassive black holes with reliable black hole spin, black hole mass, broad line region luminosity (BLR), and 1.4 GHz radio flux. The method of X-Ray Reflection Spectroscopy is used to measure the spin of a black hole (Gallo et al. 2011; Brenneman 2013; Lohfink et al. 2013; Risaliti et al. 2013; Walton et al. 2013; Reis et al. 2014; Keck et al. 2015; Buisson et al. 2018; Parker et al. 2018; Sun et al. 2018; Jiang et al. 2019; Walton et al. 2019, 2020). Meanwhile, we consider that these sources have the luminosity of broad emission lines (Grupe et al. 2004; Sugai et al. 2007; Sulentic et al. 2007; Buttiglione et al. 2010; Assef et al. 2011; Koss et al. 2017; Malkan et al. 2017; Daniel & Wyse 2018; Afanasiev et al. 2019; Kim et al. 2021). The accretion disk luminosity is estimated by using $L_{\rm disk} = 10L_{\rm BLR}$, with an average uncertainty of a factor 2 (Calderone et al. 2013; Ghisellini et al. 2014). We also calculate the radio-loudness using the ratio of the flux of 1.4 GHz to the flux of B-band, $R = S_{1.4}/S_B$ (e.g., Hao et al. 2014). In Table 1, we show the sample of supermassive black holes.

2.2. The Jet Power

The jet power of the AGN can be derived from the radio luminosity of the compact core (e.g., Merloni & Heinz 2007; Cavagnolo et al. 2010; Daly et al. 2012). Cavagnolo et al. (2010) obtained the relationship between radio luminosity and jet power using 21 giant elliptical galaxies

$$\log P_{\rm jet} = 0.75(\pm0.14)\log P_{1.4} + 1.91(\pm0.18), \quad (1)$$

where $L_{1.4}$ is the 1.4 GHz radio powers, which is estimated by the relation $P_{1.4} = 4\pi d_{\rm L}^2(1+z)^{\alpha-1}S_\nu\nu$. The S_ν is the flux density at 1.4 GHz from NASA/IPAC Extragalactic Database (NED), and the spectral index $\alpha = 0$ (e.g., Abdo et al. 2010; Komossa et al. 2018). The $P_{\rm jet}$ is in units 10^{42} erg s^{-1} and $P_{1.4}$ in units 10^{40} erg s^{-1}. The scatter for this relation is $\sigma_{1.4} = 0.78$ dex. In the sample of Cavagnolo et al. (2010), about 76%

Table 1
The Sample of Supermassive Black Holes

Name [1]	z [2]	S_ν [3]	$\log L_{\rm radio}$ [4]	$\log M/M_\odot$ [5]	j [6]	Mass/Spin Reference [7]	$\log L_{\rm BLR}$ [8]	References [9]	S_B [10]	$\log R$ [11]	$S_{\rm X-ray}$ [12]	$S_{\rm X-ray,\ Error}$ [13]
Mrk 335	0.02578	7.6 ± 0.6	38.2	7.15 ± 0.11	$0.83^{+0.09}_{-0.13}$	Pe04/Wa13	42.73	S07	5.22 ± 0.173	0.16	6.50E-07	6.90E-09
IRAS 00521-7054	0.069	36 ± 2	39.74	7.7 ± 0.09	$0.98^{+0.018}_{0.04}$	Wa19	41.56	M17	0.467 ± 0.0495	1.89	1.66E-07	0.00E+00
Mrk 359	0.0168	44 ± 0.6	38.59	6.04	$0.66^{+0.30}_{-0.54}$	ZW05/Wa13	40.84	K17	6.81 ± 0.727	0.81	5.10E-07	2.07E-08
Mrk 1018	0.043	4.3 ± 0.5	38.4	8.15	$0.58^{+0.36}_{-0.74}$	Be11/Wa13	41.92	B10	8.12 ± 1.2	−0.28	5.59E-07	7.59E-08
NGC 1365	0.00546	377 ± 13	38.54	$6.3^{+0.53}_{-0.23}$	$0.97^{+0.01}_{-0.04}$	Fa19/Ri13	40.73	M17	39.8 ± 0.79	0.98	4.55E-07	6.54E-08
3C120	0.033	3440 ± 103	41.07	$7.74^{0.20}_{-0.15}$	$0.994^{+0.004}_{-0.04}$	Pe04/Lo13	42.48	M17	2.23 ± 0.41	3.19	3.05E-06	1.53E-07
Ark120	0.0327	12.4 ± 0.6	38.62	8.18 ± 0.06	$0.64^{+0.19}_{-0.11}$	Pe04/Wa13	42.98	K17	11.5 ± 0.46	0.03	1.89E-06	1.88E-07
Mrk 79	0.022	22.2 ± 1.3	38.52	7.72 ± 0.12	$0.7^{+0.10}_{-0.10}$	Pe04/Ga11	42.12	M17	5.13 ± 0.12	0.64	1.79E-06	1.79E-07
NGC 3783	0.00973	44.6 ± 2	38.11	7.47 ± 0.08	$0.92^{+0.04}_{-0.04}$	Pe04/Br13	42.01	K17	7.7 ± 0.24	0.76	3.55E-06	1.76E-07
NGC 4151	0.0033	360 ± 10.8	38.08	7.57 ± 0.15	$0.94^{+0.05}_{-0.05}$	On14/Ke15	41.28	M17	37.4 ± 0.61	0.98	1.39E-05	6.90E-07
Mrk 766	0.01288	40.4 ± 1.9	38.32	$6.25^{+0.05}_{-0.04}$	$0.92^{+0.05}_{-0.05}$	Be06/Bu18	40.36	K17	1.58 ± 0	1.41	2.07E-06	0.00E+00
PG1229+204	0.0636	3.1 ± 0.5	38.6	7.76 ± 0.22	$0.93^{+0.06}_{-0.02}$	Ji19	42.44	K17	2.24 ± 1.31	0.14	1.75E-07	1.10E-08
IRAS13349+2438	0.108	20 ± 0.8	39.88	$8.63^{+0.09}_{-0.17}$	$0.93^{+0.03}_{-0.02}$	Pa18	44.67	A19	4.68 ± 0	0.63	2.48E-07	0.00E+00
Ark564	0.0247	29.1 ± 1	38.74	6.04	$0.96^{+0.11}_{-0.01}$	ZW05/Wa13	41.39	S07	6.27 ± 1.48	0.67	1.38E-06	0.00E+00
NGC5506	0.00608	355 ± 10	38.61	$6.7^{+0.19}_{-0.10}$	$0.93^{+0.04}_{-0.04}$	Ni09/Su18	40	K17	19.7 ± 2.1	1.26	5.78E-06	0.00E+00
IRAS09149-6206	0.0573	$16pm0$	39.22	$8^{+1.3}_{-0.3}$	$0.94^{+0.02}_{-0.07}$	Wa20/Wa20	43.64	K17	15.1 ± 0	0.03	5.86E-07	0.00E+00
RXS J1131-1231	0.654	15 ± 0	41.36	8.3 ± 0.09	$0.87^{+0.08}_{-0.15}$	Sl12/Re14	44.03	S07	0.694 ± 0	1.33	1.66E-07	0.00E+00

Note. Column (1): name; Column (2): redshift; Column (3): the 1.4 GHz flux density in units mjy; Column (4): Logarithm of 1.4 GHz radio luminosity (in units of erg s^{-1}); Column (5): Logarithm of black hole mass (in units of solar mass); Column (6): the spin of black hole; Column (7): the reference of spin and mass of black hole. Pe04 = Peterson et al. (2004); Wa13 = Walton et al. (2013); Ta12 = Tan et al. (2012); ZW05 = Zhou & Wang (2005); Be11 = Bennert et al. (2011); Va16 = Vasudevan et al. (2016); Ri13 = Risaliti et al. (2013); Lo13 = Lohfink et al. (2013); Ga11 = Gallo et al. (2011); Un20 = Ünal & Loeb (2020); On14 = Onken et al. (2014); Ke15 = Keck et al. (2015); Ta20 = Tamburini et al. (2020); Ak19 = Event Horizon Telescope Collaboration (2019); Ja19 = Jiang et al. (2019); Pa18 = Parker et al. (2018); Ni09 = Nikołajuk et al. (2009); Su18 = Sun et al. (2018); Me10 = Meléndez et al. (2010); Gr17 = Grier et al. (2017) Column (8): Logarithm of broad region luminosity (in units of erg s^{-1}); Column (9): the reference of broad line region luminosity. S07: Sulentic et al. (2007); M17 = Malkan et al. (2017); K17 = Koss et al. (2017); K18 = Komossa et al. (2018); B10 = Buttiglione et al. (2010); A19 = Afanasiev et al. (2019); Le13 = Lee et al. (2013). Column (10): the flux of optical B-band in units mjy comes from NED; Column (11): the radio-loudness; Column 12: the flux of X-ray 2–10 keV in units Jy comes from NED. Column (13): the flux error of X-ray 2–10 keV in units Jy comes from NED.

are radio-quiet AGNs (e.g., NGC 4636, NGC 5813, and NGC 5846). Therefore, Equation (1) can be used to calculate the jet power of radio-quiet AGNs. Some authors also used the above equation to estimate the jet power of radio-quiet AGNs (e..g, Cheung et al. 2016; Mezcua et al. 2019; Chen et al. 2020; Singha et al. 2023; Igo et al. 2024). We also use Equation (1) to estimate the jet power of our sample. We also note that the radio-quiet AGNs only show a compact radio core, and radio flux mainly comes from the radio core. According to the radio luminosity of 1.4 GHz (e.g., Fanaroff & Riley 1974), we find that almost all of our samples are FR I radio sources ($L_{1.4\,\mathrm{GHz}} \lesssim 10^{40.5}\,\mathrm{erg\,s^{-1}}$). This suggests that our sample has a bright core, and the 1.4 GHz radio flux mainly comes from the core. Therefore, using the radio flux of 1.4 GHz to estimate jet power will not affect our main results. In the future, when these sources have a flux of radio core, we are testing our results.

3. The Jet Model

At present, the formation mechanism of jet mainly includes the Blandford-Znajek (BZ) mechanism (Blandford & Znajek 1977), Blandford Payne (BP) mechanism (Blandford & Payne 1982) and hybrid jet model (e.g., Meier 2001; Garofalo et al. 2010), that is, the combination of BZ and BP. It is generally believed that jets and/or outflows can be accelerated and collimated by large-scale magnetic fields (e.g., Pudritz et al. 2007). Spruit & Uzdensky (2005) suggested that the large-scale magnetic field that accelerates the jet or outflow is formed by the advection of a weak external field. However, Lubow et al. (1994) found that the advection of the external field caused by the small radial velocity of geometrically thin accretion disks ($\mathrm{H/R} \ll 1$) is quite ineffective. The coronal mechanism is proposed to alleviate the problem of advection of a weak external field in thin disks (e.g., Spruit & Uzdensky 2005; Cao & Spruit 2013). Beckwith et al. (2009) found that the hot corona above the accretion disk can effectively drag the external magnetic field to move inward. Some authors found that the magnetic field of the corona can enhance the relativistic jet (e.g., Cao 2018). Our sample has high relativistic jet power, $\langle \log P_{\mathrm{jet}} \rangle = 43.50 \pm 0.35$. In this work, we, therefore, use the magnetic field of the corona above the thin accretion disk to estimate the jet power of the model. Then, the jet power of the model is compared with the observed jet power.

3.1. Magnetic Field of Corona

The corona above the accretion disk can be described by using the corona thickness H_{c} and the optical depth τ_{c} (Cao 2018). Cao (2018) estimated the magnetic field strength of the corona using the following formula

$$B = 4.37 \times 10^{8} \beta^{1/2} \tau_{\mathrm{c}}^{1/2} \tilde{H}_{\mathrm{c}}^{1/2} m^{-1/2} r^{-3/2} L_{*}^{2}\ \mathrm{Gauss} \quad (2)$$

$$r = \frac{Rc^2}{GM_{\mathrm{bh}}},\ m = \frac{M_{\mathrm{bh}}}{M_{\odot}},\ \tilde{H}_{\mathrm{c}} = \frac{H_{\mathrm{c}}}{R} \quad (3)$$

where $\tilde{H}_{\mathrm{c}}$ is the relative thickness (Cao 2018). To estimate the maximum power of the jet, $\omega_{\mathrm{F}} = 1/2$ (Ghosh & Abramowicz 1997), $\beta = 1$, $\xi_{\phi} = 1$, $\tilde{\Omega} = 1$, $\tau_{\mathrm{c}} = 0.5$, $\tilde{H}_{\mathrm{c}} = 0.5$, and the $L_{*} = L_{\mathrm{K}}(r_{\mathrm{ms}})$ are used (Cao 2018).

3.2. The Jet Model

(1) The BZ jet model.

The formula for calculating the jet power of the BZ mechanism is as follows (e.g., MacDonald & Thorne 1982; Thorne et al. 1986; Ghosh & Abramowicz 1997; Livio et al. 1999; Nemmen et al. 2007):

$$P_{\mathrm{jet}}^{\mathrm{BZ}} = \frac{1}{32} \omega_{\mathrm{F}}^{2} B_{\perp}^{2} R_{\mathrm{H}}^{2} j^{2} c, \quad (4)$$

where $B_{\perp}$ is the magnetic field strength of the black hole horizon, $B_{\perp} \approx B$, and $R_{\mathrm{H}} = [1 + (1 - j^2)^{1/2}] GM_{\mathrm{bh}}/c^2$ indicates the horizon radius. The ω_{F} is estimated by using the angular velocity of field lines Ω_{F} and the hole Ω_{H}, $\omega_{\mathrm{F}} \equiv \Omega_{\mathrm{F}}(\Omega_{\mathrm{H}} - \Omega_{\mathrm{F}})/\Omega_{\mathrm{H}}^{2}$. In order to obtain the maximal jet power of the BZ mechanism, $\omega_{\mathrm{F}} = 1/2$ is used (MacDonald & Thorne 1982).

(2) The BP jet model.

We use the following formula to calculate the jet power of the BP jet model (Livio et al. 1999; Cao 2018)

$$P_{\mathrm{jet}}^{\mathrm{BP}} \sim \frac{BB_{\phi}^{s}}{2\pi} R_{\mathrm{j}} \Omega \pi R_{\mathrm{j}}^{2}, \quad (5)$$

where B_{ϕ}^{s} is $B_{\phi}^{s} = \xi_{\phi} B$. B_{ϕ}^{s} indicates the azimuthal component of the magnetic field on the corona surface. The ratio $\xi_{\phi} \leqslant 1$ is required (Livio et al. 1999). The R_{j} indicates the radius of the jet formation area in the corona. The Ω is the angular velocity of the gas in the corona. According to Equations (2) and (5) the jet power of BP mechanism can be estimated as follows

$$P_{\mathrm{jet}}^{BP} \simeq 3.13 \times 10^{37} \xi_{\phi} \tilde{\Omega} r_{\mathrm{j}}^{-1/2} m \beta \tau_{\mathrm{c}} \tilde{H}_{\mathrm{c}}\ \mathrm{erg\,s^{-1}}. \quad (6)$$

Due to the fact that most of the released gravitational power is located in the internal region of the accretion disk with a radius $\sim 2R_{\mathrm{ms}}$ (Shakura & Sunyaev 1973), we use $R_{\mathrm{j}} = 2R_{\mathrm{ms}}$ to estimate jet power of BP model. The R_{ms} can be derived by the following formula,

$$\begin{aligned} R_{\mathrm{ms}} &= R_{\mathrm{G}}\{3 + Z_2 - [(3 - Z_1)(3 + Z_1 + 2Z_2)]^{1/2}\}, \\ Z_1 &\equiv 1 + (1 - a^2)^{1/3}[(1 + a)^{1/3} + (1 - a)^{1/3}], \\ Z_2 &\equiv (3a^2 + Z_1^2)^{1/2}, \\ R_{\mathrm{G}} &= \frac{GM_{\mathrm{bh}}}{c^2}. \end{aligned} \quad (7)$$

(3) The hybrid jet model.

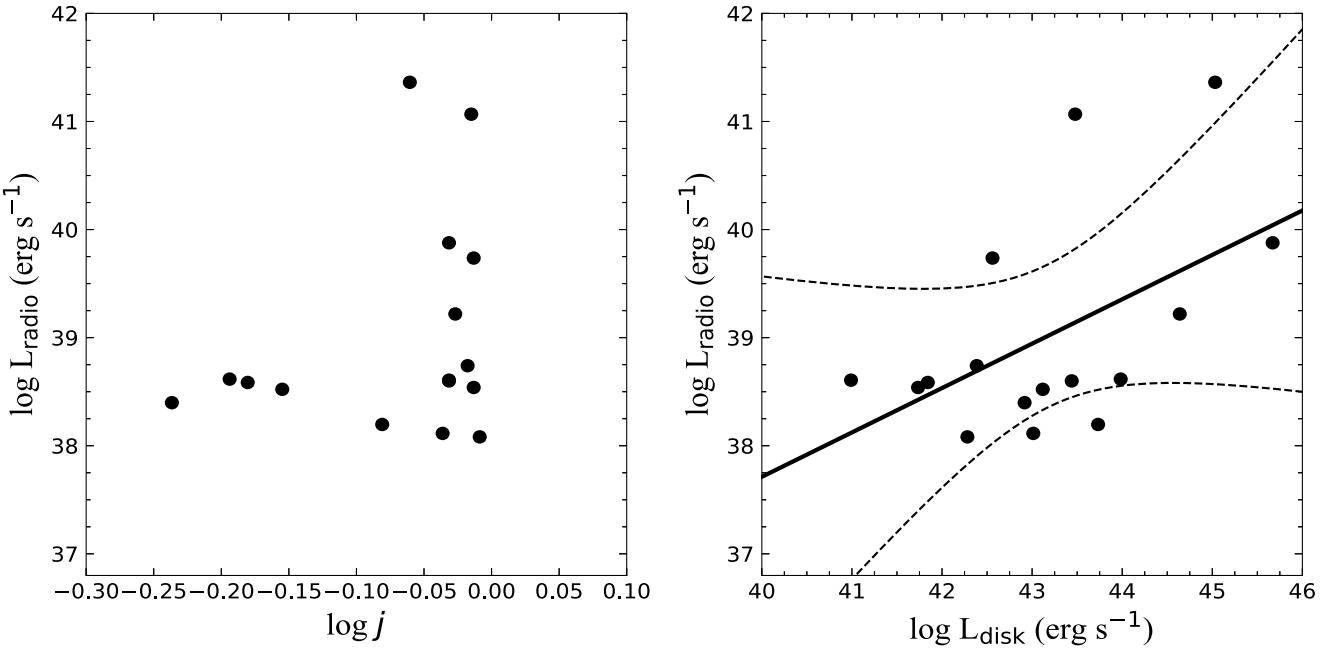

Figure 1. Relation between black hole spin (left panel) and accretion disk luminosity (right panel) and radio luminosity for supermassive black hole. The solid line is the best linear fitting. Dashed lines are the 3σ confidence band.

The hybrid model is a mixture of BZ and BP mechanisms. Garofalo et al. (2010) used the following formula to obtain the jet power of the hybrid model in the case of a thin accretion disk

$$P_{\rm jet}^{\rm Hybrid} = 2 \times 10^{47} \alpha f^2 \left(\frac{B_{\rm pd}}{10^5 G}\right)^2 \left(\frac{m}{10^9 M_\odot}\right)^2 j^2 {\rm erg\ s^{-1}}, \quad (8)$$

where $B_{\rm pd}$ is $B_{\rm pd} \simeq B$. The BZ and BP mechanisms are combined with parameters α and f. α and f is respectively given by (Garofalo 2009)

$$\alpha = \delta\left(\frac{3}{2} - j\right) \quad (9)$$

and

$$f = -\frac{3}{2}j^3 + 12j^2 - 10j + 7 - \frac{0.002}{(j-0.65)^2} + \frac{0.1}{(j+0.95)} + \frac{0.002}{(j-0.055)^2}. \quad (10)$$

The conservative value of δ is about 2.5 (Garofalo et al. 2010). α represents that the effectiveness of the BP jet is a function of the spin of the black hole, while f reflects the enhancing effect of the disk thread field on the black hole.

4. Result and Discussion

4.1. The Formation Mechanism of Jets

At present, there are three popular jet formation mechanisms, including the BZ mechanism (Blandford & Znajek 1977), BP mechanism (Blandford & Payne 1982) and hybrid model (Meier 2001; Garofalo et al. 2010). The BZ mechanism mainly extracts the rotational energy of the black hole, while the BP mechanism mainly extracts the rotational energy of the accretion disk. The hybrid model is a mixture of the BZ and BP mechanisms. In the BZ and BP mechanisms, the accretion of matter in the black hole leads to an expected relationship between the jet power and the accretion disk (Maraschi & Tavecchio 2003).

Figure 1 shows the relationship between black hole spin (left panel), accretion disk luminosity (right panel) and radio luminosity for the selected sample. From the left panel of Figure 1, we find that there is a weak correlation between radio luminosity and black hole spin for the selected sample ($r = 0.27$). We also further tested the correlation between the jet power and the black hole spin at an 84% confidence level and found that the correlation coefficient was 0.42. This result shows a moderately strong correlation between jet power and black hole spin. The best-fit equation between radio luminosity and spin is $\log L_{\rm radio} = (3.57 \pm 3.39)\log j + (39.26 \pm 0.35)$ for the selected sample. The result suggests that jet power depends on the spin of the black hole.

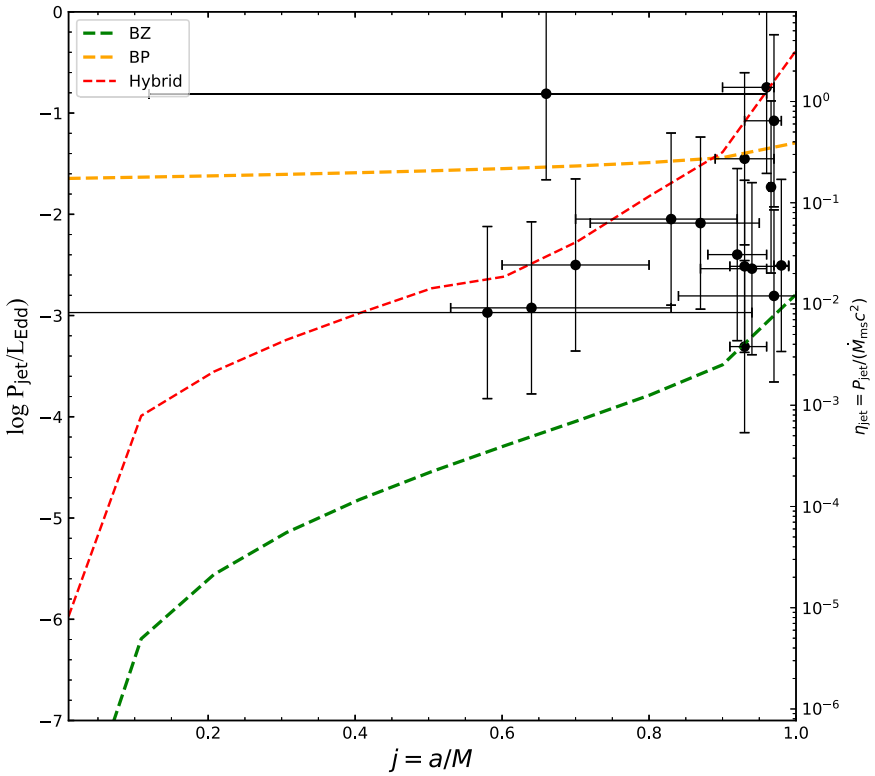

Figure 2. The jet power in Eddington units as a function of black hole spin. The orange dashed line indicates the jet power of the BP mechanism. The green dashed line indicates the BZ mechanism. The red dashed line indicates the hybrid model. The right-hand axis indicates the jet efficiency. The uncertainty of $\log P_{\rm jet}/L_{\rm Edd}$ mainly comes from $\log P_{\rm jet}$.

Some authors have found a close connection between jet and accretion (e.g., Rawlings & Saunders 1991; Ghisellini et al. 2014; Sbarrato et al. 2014; Chen et al. 2015a, 2015b; Paliya et al. 2017; Mukherjee et al. 2019; Chen et al. 2023a, 2023b, 2023c). We test this correlation. The right panel of Figure 1 shows a relation between radio luminosity and accretion disk luminosity for the selected sample. We find a significant correlation between the luminosity of the radio and the luminosity of the accretion disk for the selected sample ($r = 0.51$, $p = 0.04$). This result further proves that there is a close connection between jet and accretion for our sample. The best-fit equation between radio luminosity and accretion disk luminosity is $\log L_{\rm radio} = (0.41 \pm 0.18)\log L_{\rm disk} + (21.28 \pm 7.91)$ for the selected sample. The results in Figure 1 may further imply that the spin and accretion of the black hole enhance the relativistic jet. The jet model of our sample may be a hybrid model. We test this speculation.

The relationship between jet power in Eddington units of the model and black hole spin is shown in Figure 2. The green dashed line is the BZ mechanism. The red dashed line is the hybrid model. The orange line is the BP mechanism. From Figure 2, we find that the jet power of the BZ mechanism and the hybrid model varies with the spin of the black hole, while the jet power of the BP mechanism does not change with the spin of the black hole. The greater the spin of a black hole, the higher the efficiency of the jet, which is consistent with GRMHD simulations (Tchekhovskoy et al. 2012). The jet efficiency of the BZ model and the hybrid model is 1% and 300% when the black hole spin is 0.99, respectively. This result implies that the hybrid model plays an important role than the BZ mechanism. At the same time, we find that the jet power of the most selected sample is below the red dashed line and orange dashed line except Mrk 359, which indicates that the hybrid model can explain the jet power of almost all selected samples. We also note that Mrk 359 has a relatively low black hole mass, resulting in a high $\log P_{\rm jet}/L_{\rm Edd}$.

The properties of a corona are usually closely related to the emission of hard X-rays. If the jet model of the corona does indeed work in these supermassive black holes, one possibility is to expect a correlation between radio and hard X-ray luminosity. We check this correlation. The relation between radio and hard X-ray luminosity is shown in Figure 3. We find a significant correlation between radio luminosity and hard X-ray luminosity ($r = 0.75$, $p = 0.0009$).

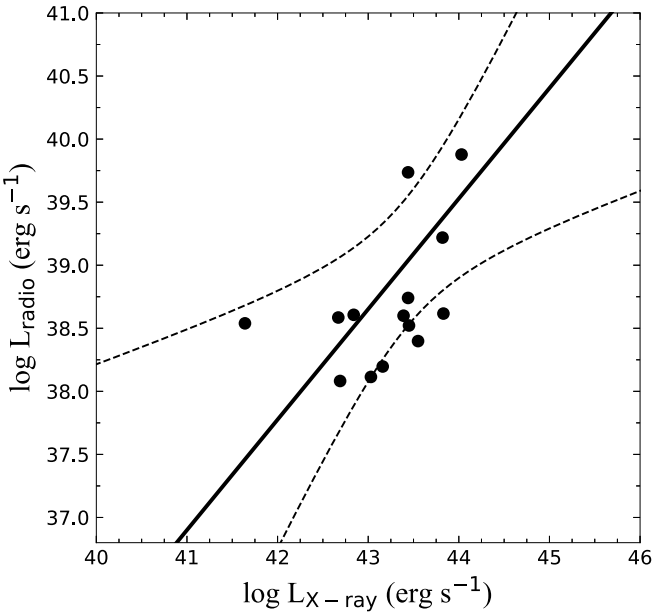

Figure 3. The radio luminosity as a function of hard X-ray luminosity for supermassive black hole. The physical meaning of the black solid and dashed lines is the same as in Figure 1.

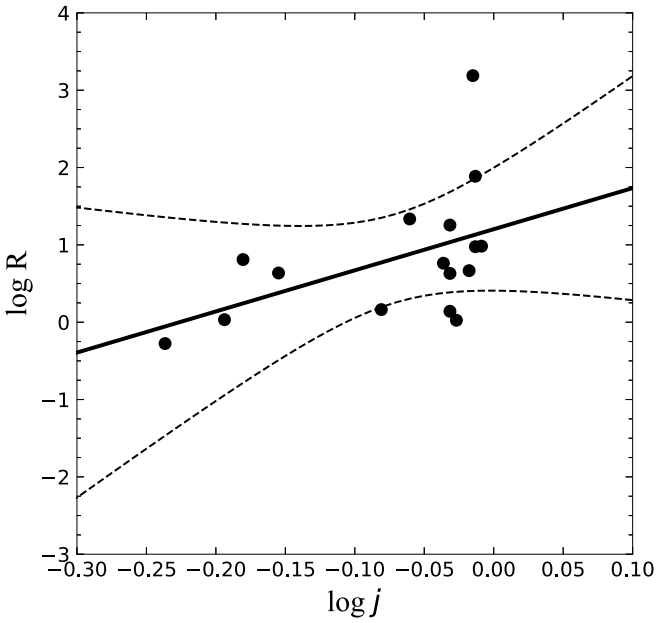

Figure 4. Relation radio-loudness and black hole spin for selected sample. The physical meaning of the black solid and dashed lines is the same as in Figure 1.

4.2. Relation Between Black Hole Spin and Radio Loudness

AGNs are divided into two types: radio-loud and radio-quiet AGNs based on radio-loudness. The origin of radio-loudness has been unclear. Some studies have found that there is an inverse correlation between radio-loudness and accretion (e.g., Sikora et al. 2007). In addition to the accretion rate, it is natural that the second physical parameter that determines the radio-loudness of AGN is related to the properties of the central black hole, such as the spin of a black hole. We test this correlation. Figure 4 shows the relation between radio-loudness and black hole spin for supermassive black holes. We find a significant between radio-loudness and spin of black holes for selected sample ($r = 0.48$, $p = 0.04$). The best-fit equation between radio radio-loudness and spin is $\log R = (5.29 \pm 2.60)\log j + (1.18 \pm 0.26)$ for the selected sample. The sources with high radio-loudness tend to have high black hole spin, which may imply that the spin of black holes can explain the dichotomy of radio-quiet and radio-loud AGNs. Tchekhovskoy et al. (2010) investigate whether the bimodal of radio-loud and radio-quiet can be due to differences in the black hole spin by using numerical simulation. They suggested that the dichotomy of radio-loud and radio-quiet can be explained by two different populations of galaxies with modestly different black hole spins. The radio-loud and radio-quiet AGN may have different merger and accretion histories, which lead to different black hole spin. The radio-loud AGN hosts in elliptical galaxies, whereas radio-quiet AGN is likely to host in spiral galaxies (Sikora et al. 2007). Volonteri et al. (2007) found that the average spin of supermassive black holes in elliptical galaxies is higher than that in spiral galaxies. The radio-loud AGN may have a higher black hole spin than radio-quiet AGN. However, we find the parameter space for the black hole spin is quite narrow (e.g., log$j$ from -0.3 to 0), where most sources have very high spin parameters and only four sources with $j \sim 0.6$–0.7. This correlation may be strongly affected by the sample selection. In the future, our results should be tested using large samples.

5. Conclusions

In this work, we study the relation between jet, accretion, and black hole spin. We also study the relation between radio-loudness and black hole spin. Our main results are as follows:

1. We find that there is a weak correlation between radio luminosity and the black hole spin for our sample. We further test the correlation between the jet power and the black hole spin at an 84% confidence level and find that the correlation coefficient was 0.42. These results imply that the jet of the supermassive black hole in our sample mainly depends on the other parameters besides black hole spin.

2. We investigate the jet power of the BZ mechanism, BP mechanism, and hybrid mechanism based on the thin disk surrounding Kerr black holes. According to the diagram of the relationship between jet power in Eddington units and black hole spin, we find that the hybrid model can explain the jet power of almost all sources.

3. There is a significant correlation between radio-loudness and black hole spin for our sample. This result may provide observational evidence for explaining radio-quiet and radio-loud dichotomy.

Acknowledgments

We are very grateful to the referee and Editor for the very helpful report. Y.C. is grateful for financial support from the National Natural Science Foundation of China (NSFC, No. 12203028). This work was supported by the research project of Qujing Normal University (2105098001/094). This work is supported by the youth project of Yunnan Provincial Science and Technology Department (202101AU070146, 2103010006). Y.C. is grateful for funding for the training Program for talents in Xingdian, Yunnan Province. Q.S.G.U. is supported by the NSFC (12121003, 12192220, and 12192222). We also acknowledge the science research grants from the China Manned Space Project with No. CMS-CSST-2021-A05. This work is supported by the NSFC (11733001, U2031201 and 12433004).

References

Abdo, A. A., Ackermann, M., Agudo, I., et al. 2010, ApJ, 716, 30
Afanasiev, V. L., Popović, L. Č., & Shapovalova, A. I. 2019, MNRAS, 482, 4985
Assef, R. J., Denney, K. D., Kochanek, C. S., et al. 2011, ApJ, 742, 93
Beckwith, K., Hawley, J. F., & Krolik, J. H. 2009, ApJ, 707, 428
Bennert, V. N., Auger, M. W., Treu, T., Woo, J.-H., & Malkan, M. A. 2011, ApJ, 726, 59
Blandford, R. D., & Payne, D. G. 1982, MNRAS, 199, 883
Blandford, R. D., & Znajek, R. L. 1977, MNRAS, 179, 433
Brenneman, L. 2013, Measuring the Angular Momentum of Supermassive Black Holes (New York: Springer)
Buisson, D. J. K., Parker, M. L., Kara, E., et al. 2018, MNRAS, 480, 3689
Buttiglione, S., Capetti, A., Celotti, A., et al. 2010, A&A, 509, A6
Calderone, G., Ghisellini, G., Colpi, M., & Dotti, M. 2013, MNRAS, 431, 210
Cao, X. 2018, MNRAS, 473, 4268
Cao, X., & Spruit, H. C. 2013, ApJ, 765, 149
Cavagnolo, K. W., McNamara, B. R., Nulsen, P. E. J., et al. 2010, ApJ, 720, 1066
Chen, S., Järvelä, E., Crepaldi, L., et al. 2020, MNRAS, 498, 1278
Chen, Y., Gu, Q., Fan, J., et al. 2023a, MNRAS, 519, 6199
Chen, Y., Gu, Q., Fan, J., et al. 2023b, ApJS, 265, 60
Chen, Y., Gu, Q., Fan, J., et al. 2023c, ApJS, 268, 6
Chen, Y.-Y., Zhang, X., Xiong, D., & Yu, X. 2015a, AJ, 150, 8
Chen, Y. Y., Zhang, X., Zhang, H. J., & Yu, X. L. 2015b, MNRAS, 451, 4193
Cheung, E., Bundy, K., Cappellari, M., et al. 2016, Natur, 533, 504
Cui, Y., Hada, K., Kawashima, T., et al. 2023, Natur, 621, 711
Daly, R. A., Sprinkle, T. B., O'Dea, C. P., Kharb, P., & Baum, S. A. 2012, MNRAS, 423, 2498
Daniel, K. J., & Wyse, R. F. G. 2018, MNRAS, 476, 1561
Event Horizon Telescope Collaboration, Akiyama, K., Alberdi, A., et al. 2019, ApJL, 875, L1
Fanaroff, B. L., & Riley, J. M. 1974, MNRAS, 167, 31P
Fender, R. P., Gallo, E., & Russell, D. 2010, MNRAS, 406, 1425
Gallo, L. C., Miniutti, G., Miller, J. M., et al. 2011, MNRAS, 411, 607
Garofalo, D. 2009, ApJ, 699, 400
Garofalo, D., Evans, D. A., & Sambruna, R. M. 2010, MNRAS, 406, 975
Ghisellini, G. 2006, in Proc. of the VI Microquasar Workshop: Microquasars and Beyond, (Trieste: SISSA), 27.1
Ghisellini, G., Tavecchio, F., Maraschi, L., Celotti, A., & Sbarrato, T. 2014, Natur, 515, 376
Ghosh, P., & Abramowicz, M. A. 1997, MNRAS, 292, 887
Grier, C. J., Pancoast, A., Barth, A. J., et al. 2017, ApJ, 849, 146
Grupe, D., Mathur, S., Wilkes, B., & Elvis, M. 2004, AJ, 127, 1
Hao, H., Sargent, M. T., Elvis, M., et al. 2014, arXiv:1408.1090
Ho, L. C., Rudnick, G., Rix, H.-W., et al. 2000, ApJ, 541, 120
Igo, Z., Merloni, A., Hoang, D., et al. 2024, A&A, 686, A43
Jiang, J., Walton, D. J., Fabian, A. C., & Parker, M. L. 2019, MNRAS, 483, 2958
Keck, M. L., Brenneman, L. W., Ballantyne, D. R., et al. 2015, ApJ, 806, 149
Kim, M., Barth, A. J., Ho, L. C., & Son, S. 2021, ApJS, 256, 40
Komossa, S., Xu, D. W., & Wagner, A. Y. 2018, MNRAS, 477, 5115
Koss, M., Trakhtenbrot, B., Ricci, C., et al. 2017, ApJ, 850, 74
Lee, N., Sanders, D. B., Casey, C. M., et al. 2013, ApJ, 778, 131
Livio, M., Ogilvie, G. I., & Pringle, J. E. 1999, ApJ, 512, 100
Lohfink, A. M., Reynolds, C. S., Jorstad, S. G., et al. 2013, ApJ, 772, 83
Lubow, S. H., Papaloizou, J. C. B., & Pringle, J. E. 1994, MNRAS, 267, 235
MacDonald, D., & Thorne, K. S. 1982, MNRAS, 198, 345
Malkan, M. A., Jensen, L. D., Rodriguez, D. R., Spinoglio, L., & Rush, B. 2017, ApJ, 846, 102
Maraschi, L., & Tavecchio, F. 2003, ApJ, 593, 667
Meier, D. L. 2001, ApJL, 548, L9
Meléndez, M., Kraemer, S. B., & Schmitt, H. R. 2010, MNRAS, 406, 493
Merloni, A., & Heinz, S. 2007, MNRAS, 381, 589
Mezcua, M., Suh, H., & Civano, F. 2019, MNRAS, 488, 685
Mukherjee, S., Mitra, K., & Chatterjee, R. 2019, MNRAS, 486, 1672
Narayan, R., & McClintock, J. E. 2012, MNRAS, 419, L69
Nemmen, R. S., Bower, R. G., Babul, A., & Storchi-Bergmann, T. 2007, MNRAS, 377, 1652
Nikołajuk, M., Czerny, B., & Gurynowicz, P. 2009, MNRAS, 394, 2141
Onken, C. A., Valluri, M., Brown, J. S., et al. 2014, ApJ, 791, 37
Paliya, V. S., Marcotulli, L., Ajello, M., et al. 2017, ApJ, 851, 33
Parker, M. L., Matzeu, G. A., Guainazzi, M., et al. 2018, MNRAS, 480, 2365
Peterson, B. M., Ferrarese, L., Gilbert, K. M., et al. 2004, ApJ, 613, 682
Pudritz, R. E., Ouyed, R., Fendt, C., & Brandenburg, A. 2007, in Protostars and Planets V, ed. B. Reipurth, D. Jewitt, & K. Keil (Tucson, AZ: Univ. Arizona Press), 277
Rawlings, S., & Saunders, R. 1991, Natur, 349, 138
Reis, R. C., Reynolds, M. T., Miller, J. M., & Walton, D. J. 2014, Natur, 507, 207
Risaliti, G., Harrison, F. A., Madsen, K. K., et al. 2013, Natur, 494, 449
Sbarrato, T., Padovani, P., & Ghisellini, G. 2014, MNRAS, 445, 81
Shakura, N. I., & Sunyaev, R. A. 1973, A&A, 24, 337
Sikora, M., Stawarz, Ł., & Lasota, J.-P. 2007, ApJ, 658, 815
Singha, M., Winkel, N., Vaddi, S., et al. 2023, ApJ, 959, 107
Spruit, H. C., & Uzdensky, D. A. 2005, ApJ, 629, 960
Steiner, J. F., McClintock, J. E., & Narayan, R. 2013, ApJ, 762, 104
Sugai, H., Kawai, A., Shimono, A., et al. 2007, ApJ, 660, 1016
Sulentic, J. W., Bachev, R., Marziani, P., Negrete, C. A., & Dultzin, D. 2007, ApJ, 666, 757
Sun, S., Guainazzi, M., Ni, Q., et al. 2018, MNRAS, 478, 1900
Tamburini, F., Thidé, B., & Della Valle, M. 2020, MNRAS, 492, L22
Tan, Y., Wang, J. X., Shu, X. W., & Zhou, Y. 2012, ApJL, 747, L11
Tchekhovskoy, A., McKinney, J. C., & Narayan, R. 2012, JPhCS, 372, 012040
Tchekhovskoy, A., Narayan, R., & McKinney, J. C. 2010, ApJ, 711, 50
Thorne, K. S., Price, R. H., & MacDonald, D. A. 1986, Black Holes: The Membrane Paradigm (New Haven, CT: Yale Univ. Press)
Ünal, C., & Loeb, A. 2020, MNRAS, 495, 278
Vasudevan, R. V., Fabian, A. C., Reynolds, C. S., et al. 2016, MNRAS, 458, 2012
Volonteri, M., Sikora, M., & Lasota, J.-P. 2007, ApJ, 667, 704
Walton, D. J., Alston, W. N., Kosec, P., et al. 2020, MNRAS, 499, 1480
Walton, D. J., Nardini, E., Fabian, A. C., Gallo, L. C., & Reis, R. C. 2013, MNRAS, 428, 2901
Walton, D. J., Nardini, E., Gallo, L. C., et al. 2019, MNRAS, 484, 2544
Zamaninasab, M., Clausen-Brown, E., Savolainen, T., & Tchekhovskoy, A. 2014, Natur, 510, 126
Zhou, X.-L., & Wang, J.-M. 2005, ApJL, 618, L83